^{99m}Tc-MDP as an imaging tool to evaluate the *in vivo* biodistribution of solid lipid nanoparticles

Vusani Mandiwana[ab], Lonji Kalombo[a], Anne Grobler[b], Jan Rijn Zeevaart[bc]

[a] Centre of Polymers and Composites, Council for Scientific and Industrial Research, P.O. Box 395, Pretoria, 0001, South Africa E-mail: VMandiwana@csir.co.za; LKalombo@csir.co.za

[b] DST/NWU Preclinical Drug Development Platform, North-West University, Private Bag X6001, Potchefstroom, 2520, South Africa E-mail: Anne.Grobler@nwu.ac.za

[c] Radiochemistry, South African Nuclear Energy Corporation, Pelindaba, P.O. Box 582, Pretoria, 0001, South Africa E-mail: janrijn.zeevaart@necsa.co.za

Author to whom correspondence should be addressed; Centre of Polymers and Composites, CSIR, PO Box 395, Pretoria, 0001, South Africa; E-mail: VMandiwana@csir.co.za; Tel.: +27 12 841 2985;
Fax: +27 12 841 3553

ABSTRACT

The aim of this study was to establish the *in vivo* uptake and tissue distribution of ^{99m}Tc-MDP-encapsuated Solid Lipid Nanoparticles (SLNs) post administration. Radioactive ^{99m}Tc-MDP encapsulated into SLNs was administered to rats to trace their biodistribution through imaging and *ex vivo* studies. As expected IV injected ^{99m}Tc-MDP exhibited predominant visual bone uptake and a high localisation of particles in the kidneys (3.87%ID/g) followed by bone (2.66%ID/g). IV administered ^{99m}Tc-MDP encapsulated by SLN showed similar uptake than ^{99m}Tc-MDP. Orally administrated ^{99m}Tc-MDP showed no uptake in any organs except the GI-tract while orally administered ^{99m}Tc-MDP-SLN showed distinct transfer of ^{99m}Tc-MDP from the GI tract with measurable levels in the kidneys and bone.

Keywords: *Biodistribution, in vivo imaging, SLNs, ^{99m}Tc-MDP*

1. Introduction

Solid lipid nanoparticles (SLNs) are made from emulsions of lipids which are in the solid state at room temperature (Wissing *et al.* 2004) and wherein the active compound can be encapsulated either in the shell or in the core (Mehnert and Mäder, 2001; Parveen *et al*., 2012). SLNs can be made up of triglycerides, complex glyceride mixtures or waxes, and are stabilised by surfactants (Wissing *et al.* 2004). The advantages of SLNs include their versatility to nano-encapsulate extremely hydrophobic as well as hydrophilic drugs (Almeida & Souto 2007; Lasoń & Ogonowski, 2011) and to provide various rates of drug release in a controlled fashion (Ekambaram *et al.*, 2012). Nanoparticulate delivery systems such as SLNs have gained attention because of their biodegradability properties as well as low toxicity (Ekambaram *et al.*, 2012). The size and loading of the nanoparticles can easily be manipulated to provide enhanced control over drug delivery (Munireddy *et al*. 2012). SLNs can be used to provide enhanced bioavailability of drugs via modification of the dissolution rate and/or improved tissue distribution (Ramteke *et al.*, 2012). To improve on the current inadequate control of malaria, the Drug Delivery and Encapsulation research group at the Council for Scientific and Industrial Research (CSIR) is developing nano-sized delivery systems containing anti-malaria drugs that aim to enable entry, slow release and retention of the drugs in the cells for longer periods and to enhance bioavailability. The aim is to reduce the drug dose frequency from daily intake to once-off treatment or a weekly administration. Enhanced *in viv*o drug biodistribution is important in improving the efficacy of these therapeutic drugs and in limiting their potential side effects. Monitoring the accumulation of a therapeutic formulation in specific organs or tissue in real-time can allow scientists to optimize the formulations to enhance their biodistribution properties. One of the methods used in tracking particle uptake or biodistribution involves the use of radiolabelled nanoparticles.

A powerful feature of nuclear molecular imaging involves the evaluation of drug delivery systems *in vivo* (Chopra, 2010). It is a technique that uses external detectors such as gamma (γ) cameras to capture and form images from the radiation emitted by radiopharmaceuticals post administration (Bhatnagar *et al.*, 2000). The use of techniques adapted from clinical radiopharmacy and nuclear medicine facilities allow delivery systems to be radiolabelled and their release, biodistribution and uptake may be visualized *in vivo* (Perkins and Frier, 2004). For example, by tagging a drug molecule, peptide or protein with a radiotracer, its site of release

and distribution can be studied. Imaging technology uses suitable γ emitting radionuclides, such as technetium-99m (^{99m}Tc), indium-111 (^{111}In), iodine-123 (^{123}I) and samarium-153 (^{153}Sm), which may be imaged using a γ camera (Yeong *et al.*, 2011). An advantage of these techniques is that the *in vivo* distribution and kinetics of a radiolabelled pharmaceutical formulation may be quantified; as a result a correlation between the observed pharmacological effects and the specific site of delivery may be made (Chopra, 2010). However, a majority of formulation laboratories lack the resources and expertise for suitable labelling techniques of nanoparticles for biodistribution studies. Unfortunately, radiolabelling and biodistribution formulation studies are time-dependent because radioactive material such as ^{99m}Tc decays within a few hours. Therefore the time when the radiopharmaceutical formulation is quantified is critical and has to be allowed for.

This study was part of a bigger long term study to investigate delivery systems for diagnostic imaging. ^{153}Sm-PLGA nanoparticles (Mandiwana *et al.,* 2015) were a proof of concept for a 48 h biodistribution study. From the imaging results obtained in that study it became apparent that the localisation was much faster shown by the 48 h and that even before 24 h (termination point) localisation became stagnant. SLN was developed with the use of a microemulsion where distribution happens much quicker, therefore the selection of ^{99m}Tc was believed to be sufficient in this study.

The aim of the study reported here was to (i) determine the biodistribution of Technetium-99m -methylene diphosphonate (^{99m}Tc-MDP)-encapsulated SLNs, (ii) to establish the *in vivo* uptake and localisation of ^{99m}Tc-MDP-SLNs and (iii) their release profiles in healthy rats post oral and intravenous (IV) administration. Technetium-99m is a radioactive γ emitting radio-element that has a half-life of 6 h and ^{99m}Tc-labelled agents are used as imaging agents (Sheets & Wang, 2011). ^{99m}Tc-MDP is a commonly used bone-imaging agent because it accumulates in bone (Mitterhauser *et al.* 2004). ^{99m}Tc has a γ photon emission of 140 KeV, which is an advantage for effective and safe imaging from a patient's perspective but also provides effective imaging in preclinical trials. ^{99m}Tc-MDP was chosen as it is a widely available radiopharmaceutical but more importantly it gives a distinct biodistribution that is easily recognisable i.e. bone uptake and fast clearance of the non-targeting remainder through the kidneys into the urine (Truluck, 2007; Geskovski *et al.,* 2013). Furthermore the uptake of IV administrated ^{99m}Tc-MDP is well known. For orally administrated ^{99m}Tc-MDP no uptake from the gut will occur. Therefore ^{99m}Tc-MDP provides an excellent positive and negative control for this study in which the

effect of the SLN upon the biodistribution (oral and IV) is determined. The first step in this study was the design and production of radiolabelled ^{99m}Tc-MDP encapsulated SLNs smaller than 500 nm. This delivery system was intended to be radiolabelled by encapsulating a radiotracer (^{99m}Tc) instead of an anti-malaria drug compound. The conventional method of nanoparticle formulation involves encapsulating a drug into the nanoparticle shell instead of a radionuclide. This was done with the aim of tracking the uptake, biodistribution and localisation of these nanoparticulate delivery systems in Sprague Dawley rats.

2. Materials and methods

2.1 Materials

^{99m}Tc was eluted from a ^{99}Mo/^{99m}Tc generator (1.02 mCi/ml, NTP, Pelindaba, Necsa, South Africa). Methylene diphosphonate (MDP) was also obtained from NTP (NTP, Pelindaba, Necsa, South Africa). Polyvinyl alcohol (PVA), hydrolysed 87-89%, Mw 13 000-23 000, Tween 20 (polyethylene glycol sorbitan monolaurate), Dichloromethane (DCM), ACS reagent ≥99.5% and Methanol 99.5% were purchased from Sigma-Aldrich, Germany. Surfynol 104 PG 50 surfactant was purchased from Air Products and Chemicals. Biogapress Vegetal BM 297ATO, glyceryl distearate was purchased from Gattefossé (Saint-Priest, Cedex, France). Ketamine/ Xylazine was purchased from Phoenix Pharmaceutical (Baden-Wuerttemberg, Germany).
Water used for the preparation of all solutions and emulsions was distilled and de-ionized.

2.2.1 Preparation of a ^{99m}Tc-MDP complex

Using aseptic techniques and working in a laminar flow cabinet, ^{99m}Tc contained in a 10 cm^3 vial was added to a commercially available MDP kit (10 mg medronic acid) which was obtained from NTP to prepare a ^{99m}Tc-MDP complex. As per package insert instructions the contents were allowed to stand for 5 min at room temperature to form a ^{99m}Tc-MDP complex. The ^{99m}Tc becomes attached to a MDP ligand, a process referred to as radiolabelling, designed to localize in bone tissue.

2.2.2 Preparation of ^{99m}Tc-MDP solid lipid nanoparticles

The preparation of SLNs involved binding ^{99m}Tc to MDP by mixing gently to form a ^{99m}Tc-MDP complex. This radioactive complex was then dispersed in an emulsion containing lipids (glyceryl distearate), surfactant (surfynol 104 PG 50) and alcohol (dichloromethane) which was mixed at high speeds. The homogenized emulsion was then transferred into a PVA 2 %w/v aq. solution and further homogenized at 35 000 rpm for 10 min using the Stuart SHM1 high speed homogenizer (Bibby Scientific Ltd. Stone, Staffordshire, ST15 OSA, United Kingdom). The resulting water in oil-in-water (w/o/w) double emulsion was left to stand for 1 hour to allow the dichloromethane solvent to evaporate.

2.3 Characterisation

2.3.1 Quality control of ^{99m}Tc-MDP

2.3.1.1 Instant thin layer chromatography

Instant thin layer chromatographic (ITLC) assays were performed to determine whether the ^{99m}Tc and MDP had formed a complex before encapsulation in the SLNs. ITLC assays of ^{99m}Tc-MDP complex, ^{99m}Tc-MDP solid lipid nanoparticles and technetium free MDP solid lipid nanoparticle compounds were run on Non-ultraviolet (UV) ITLC silica gel paper, UV ITLC silica gel paper and fibreglass ITLC paper strips respectively. These compounds were spotted at the origin of each ITLC paper and run in a 10 ml solution of 10% methanol in saline. The resulting compounds were viewed under a UV light. Each strip was then cut in half, placed in plastic pockets and labelled to quantify the radioactivity. These were placed and read individually for radioactivity in a dose calibrator (Capintec, Inc, Ramsey, NJ, USA) as well as a MCA scintispec well counter. Although it would have been better to use two solvent systems the ^{99m}Tc-MDP was prepared from commercially available kit vials which should ensure adequate radiolabelling takes place each time. Hence the single solvent system was deemed sufficient in this study.

2.3.2 Characterisation of nanoparticle for particle size and surface charge

For optimising and characterisation purposes, SLNs were encapsulated with MDP without ^{99m}Tc. These were characterized for size and Zeta potential via dynamic laser scattering and Laser Doppler Velocity, respectively by using Malvern Zetasizer Nano ZS (Malvern

instruments, Worcestershire, United Kingdom). For each sample, one drop of MDP solid lipid nanoparticles, were suspended in distilled water, then sonicated for a few minutes and introduced into a U-shape Zeta cell. Each sample was measured in triplicate to determine the Zeta potential.

2.4 In vivo animal studies

Healthy female, inbred Sprague Dawley rats, weighing between 280 and 390 g were selected and housed under standard environmental conditions at an ambient temperature of 25 °C. The rats were cared for and supplied with food and water ad libitum. The rats were allowed one week to acclimatize before the commencement of the study. The rats received a unique ear mark; left ear for individual mark and right ear for group mark. Ethics approval was obtained for this study from the Ethics Committee for Research on Animals (ECRA), Tygerberg, Cape Town, South Africa, Ethics number ECRA 01/13.

2.5 Biodistribution and Imaging study

To obtain scintigraphic images of orally and intravenously administered radiolabelled particles, the rats were anaesthetised with Ketamine/ Xylazine (90/10 mg/kg). Twelve rats were assigned at random into two groups of six rats each. Further grouping included assigning the six rats each to ^{99m}Tc-MDP encapsulated SLN (^{99m}Tc-MDP-SLN) and ^{99m}Tc-MDP control, three rats for oral and the other four for intravenous administration (IV). Immediately after receiving anaesthesia and radiolabelled nanoparticles, the rats were positioned under the gamma camera collimator (Infinia SPECT/CT, GE Healthcare, Salt Lake City, Utah and Lawrence, Massachusetts, USA) in ventral decubitas. The rats were injected IV with an average volume of 200 µl or orally administered 500 µl dose of radioactive nanoparticles with an activity of 13.50-37.74 MBq. Acquisition of dynamic images (120 s per frame) was recorded for the first 15 min and static images at 1, 2, 3 and 4 h. Regions of interest (ROIs) were drawn on the images of the liver, stomach, bladder, intestines and tail to obtain time activity curves from the dynamic imaging study. Data for the ROIs, which were decay corrected, were obtained from the static images. After acquisition of images, the rats were sacrificed by intravenous administration of 100 mg sodium pentobarbital/ kg. Several organs, including the heart, lungs, liver, spleen, pancreas, stomach, intestines, kidneys, bladder, muscle, skin, bone, tail and blood were immediately removed after sacrificing euthanization of the rats. Each organ was weighed

and the radioactivity was measured using a Capintec well type counter (Capintec, Inc, Ramsey, NJ, USA) as well as a MCA scintispec well counter.

2.6 Ex vivo Biodistribution study

To determine the biodistribution of the SLNs, radioactively encapsulated particles were orally and intravenously administered to rats. Sixteen rats were assigned at random into four groups of four rats per group. These were further grouped into two groups per nanoparticle sample for the ^{99m}Tc-MDP-SLN and ^{99m}Tc-MDP control. The ventral tail artery of all rats was catheterized under Ketamine/ Xylazine (90/10 mg/kg) anaesthesia immediately before the study. Additionally, lateral tail veins were catheterized for all the rats which were administered radiolabelled nanoparticle compounds intravenously. The catheter was then removed after intravenous administration. One dose of each radiolabelled nanoparticle compound was administered either via oral route (500 µl in saline) using a 22G feeding needle attached to a 1 ml syringe or via intravenous route (200 µl in saline) through a catheterized tail vein. One rat was euthanized per time point through intravenous administration of 100 mg sodium pentobarbital/ kg. The heart, lungs, liver, spleen, pancreas, stomach, intestines, kidneys, bladder, muscle, skin, bone, tail and blood were immediately removed after killing the rats. Each organ was then contained in a test tube, weighed and the radioactivity was measured using a Capintec well type counter (Capintec, Inc, Ramsey, NJ, USA) as well as a MCA scintispec well counter. Three dilutions of the radioactive solution were made to correlate counts with activity measured in MBq.

3. Results and discussion

3.1 Quality control of radiopharmaceuticals

3.1.1 Instant thin layer chromatography

According to the results in Table 1, a complex was formed between the ^{99m}Tc and the MDP ligand. The ^{99m}Tc-MDP complex reported activity values of 0.1 (2.20%) and 0.4 (5.42%) MBq at the origin of the fiberglass and UV sheets respectively. The activities at the front were 4.53 (99.88%) and 7.34 (99.46%) MBq on the fiberglass and UV sheets respectively. Labelling

efficiency and stability of the ^{99m}Tc-MDP nanoparticle complex was also assessed using fiberglass, non-UV and UV sheets. Values of 0, 0.1 (3.50%) and 0 MBq were recorded at the origin of the fiberglass, non-UV and UV sheets respectively. The activities at the front were 0.9 (100%), 2.85 (99.65%) and 3.86 (100%) MBq on the fiberglass, non-UV and UV sheets respectively. A zero value at the origin could imply that a 100% complex was formed between the two compounds (Geskovski *et al*., 2013). The radioactivity of nanoparticulate complexes was generally lower than that of free ^{99m}Tc-MDP complexes. These results don't however prove that the ^{99m}Tc-MDP complex is encapsulated in the ^{99m}Tc-MDP solid lipid nanoparticle.

Table 1 QC results of radiopharmaceuticals

	Radioactivity (MBq) Paper type		
	Fibreglass	Al: Non-UV	Al: UV
^{99m}Tc-MDP			
Origin	0.1		0.4
Front	4.53		7.34
^{99m}Tc-MDP-SLN			
Origin	0	0.1	0
Front	0.9	2.85	3.86

*Al: aluminium, Non-UV: non-ultraviolet, UV: ultraviolet

3.2 Characterization

3.2.1 Particle size and Zeta potential

Optimization of ^{99m}Tc-MDP-SLN emulsions yielded a slightly higher polydispersity index of ≥0.5 and a size range between 150 and 450 nm. The Zeta potential was between -2 and -30 mV. The ^{99m}Tc-MDP-SLNs had an average PDI of 0.245 and particles sizes of 260 ± 2.66 nm and 252 ± 7.89 with a Zeta potential of -15 and -12.36 (Table 2). Zeta potentials between -5 and -15 mV are in a region where a limited degree of particle aggregation could occur (Parhi and Suresh, 2012). Thus particle aggregation is less likely to occur for nanoparticles with a high Zeta potential due to electric repulsion (Parhi and Suresh, 2012). The Zeta potential of these emulsions may carry a negative charge in relation to its surroundings as a result of the ingredients added.

Table 2 Size and Zeta potential of ^{99m}Tc-MDP solid lipid nanoparticles

No.	Size (nm)	PDI	Zeta potential (mV)
1	260.70 ± 2.66	0.26 ± 0.10	-15.00 ± 0.55
2	252.10 ± 7.89	0.23 ± 0.08	-12.30 ± 0.36

*PDI: polydispersity index, nm: nanometres, mV: millivolts

3.3 In vivo biodistribution studies

3.3.1 Imaging and biodistribution assays

Figure 1 shows a comparative distribution of ^{99m}Tc-MDP and ^{99m}Tc-MDP-SLN observed 4 h post oral and intravenous administration. There was however, a difference between the oral and intravenous biodistribution observed. The main difference was the amount of radioactivity and the wider biodistribution of the nanoparticles as compared to the control compounds. Looking at the images, it indicates that SLNs change the distribution of ^{99m}Tc-MDP.

Both ^{99m}Tc-MDP and ^{99m}Tc-MDP-SLNs (oral) showed a similar biodistribution where both compounds were absorbed in the stomach, spleen and liver. The main difference between orally administered ^{99m}Tc-MDP and orally administered ^{99m}Tc-MDP-SLN is that the latter is taken up from the gut and transported to other areas in the body such as bone – the target of ^{99m}Tc-MDP. The ^{99m}Tc-MDP-SLN formulation thus facilitates the transfer of ^{99m}Tc-MDP across the gut membrane into the blood stream with subsequent distribution to the target organ of ^{99m}Tc-MDP i.e. bone.

When ^{99m}Tc-MDP is injected intravenously, its biodistribution is dependent on the blood flow and the uptake reflects the rate of new bone formation (Truluck, 2007). This radiotracer accumulates in the inorganic hydroxyapatite crystal component of bone. It is therefore normal to see the uptake of the radiotracer throughout the entire skeleton (Truluck, 2007). The radiotracer ^{99m}Tc-MDP undergoes urinary excretion and activity can be seen in the kidneys,

ureters and bladder (Truluck, 2007). Symmetric uptake of ^{99m}Tc-MDP throughout the skeleton is the expected appearance of a normal bone scan of the injected radiotracer.

In Fig 1, very little difference between IV administered ^{99m}Tc-MDP and IV administered ^{99m}Tc-MDP-SLN is observable. However at 4h the bone uptake of the latter is less while the amount in the kidneys and bladder is higher perhaps indicating a slower release from the emulsion. The biodistribution data (Fig. 3) shows no statistical difference for bone uptake between the two formulations.

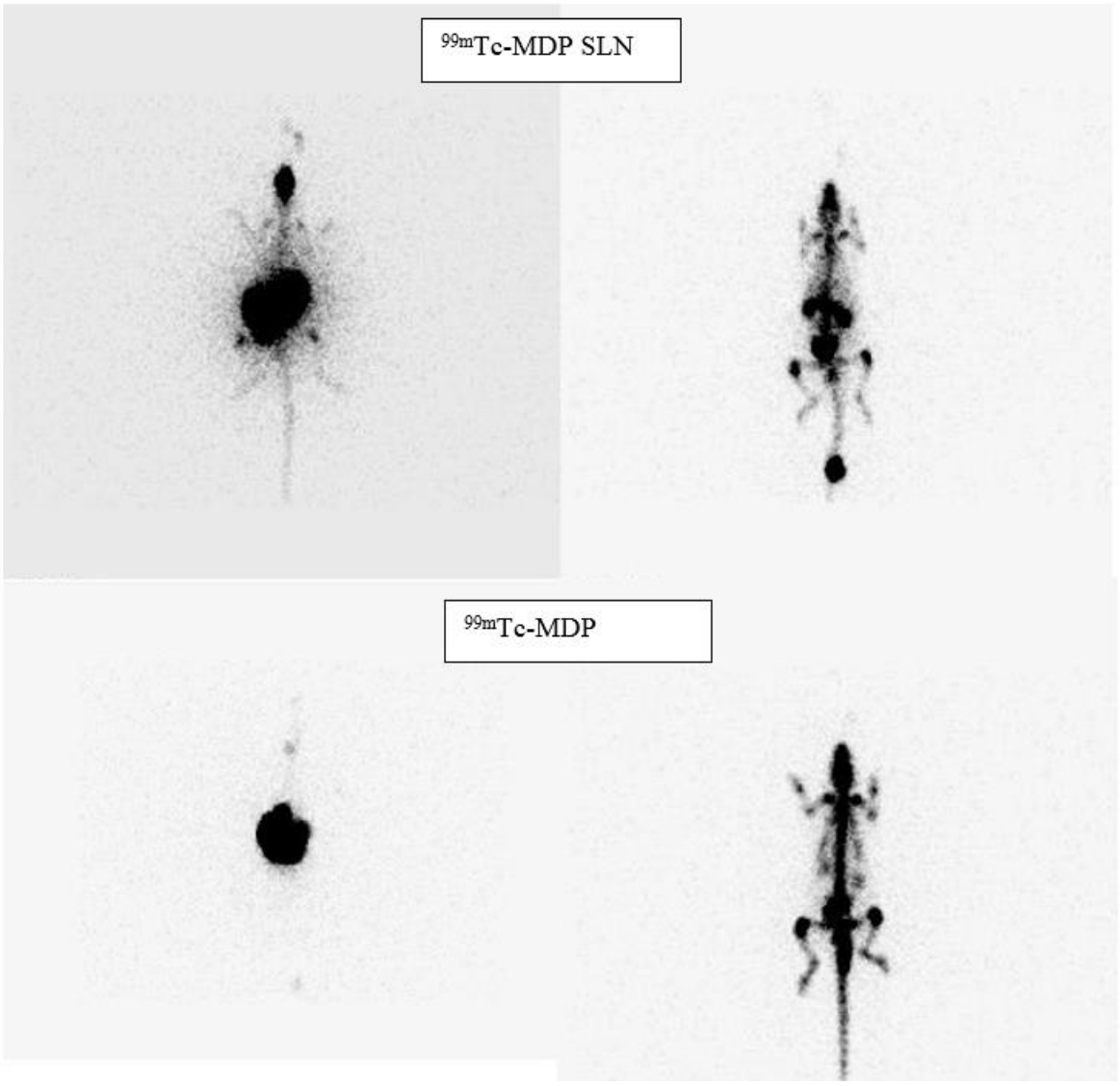

A **B**

Fig. 1. Static scintigraphic images of orally (a) and intravenously (b) administered radioactive ^{99m}Tc-MDP-SLNs and the control ^{99m}Tc-MDP at 4 h

After oral ingestion of ^{99m}Tc-MDP-SLNs, the emulsion distributed to all the major organs (Figure 2). The highest deposition (reported as %ID/g) of the ^{99m}Tc-MDP-SLNs was observed in the kidneys (8.50%ID/g), stomach (8.04%ID/g), bone (3.51%ID/g) and small intestines (3.39%ID/g). The least deposition of ingested nanoparticles was reported in the heart (0.12%ID/g) and spleen (0.13%ID/g). The oral control group ^{99m}Tc-MDP reported great localisation in the large intestines (7.08%ID/g), kidneys (1.71%ID/g), small intestines (1.46%ID/g) and stomach (1.10%ID/g). The liver (0.24%ID/g) and spleen (0.42%ID/g) are the organs which composed of the least amount of ^{99m}Tc-MDP deposition. A large amount of orally administered ^{99m}Tc-MDP was not absorbed; therefore a large amount of it accumulated and was observed in the large intestine after the 6 h duration of the study. Therefore, orally administered ^{99m}Tc-MDP was excreted via the large intestine. SLNs appeared to enhance intestinal absorption of ^{99m}Tc-MDP. SLNs were observed in bone as well because there was more absorption from the small intestine which also facilitated more absorption in bone.

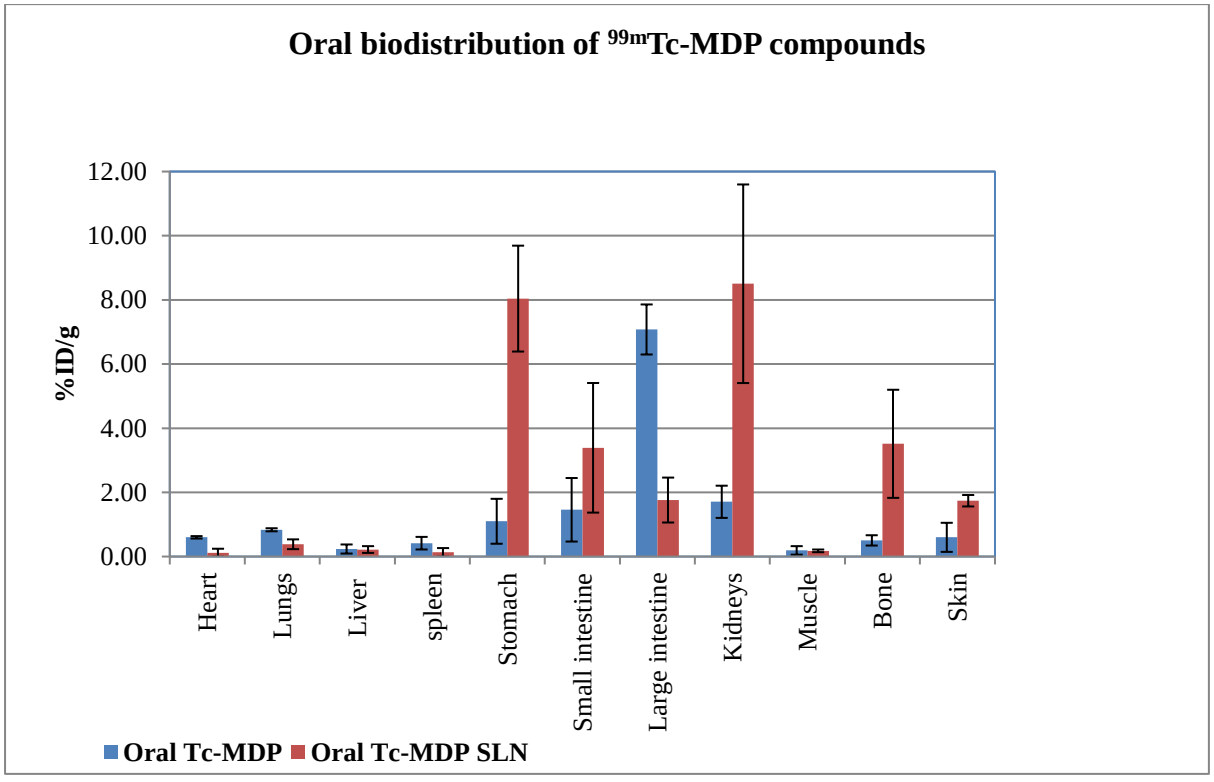

Fig. 2. The *in vivo* biodistribution of orally administered ^{99m}Tc-MDP solid lipid nanoparticles and ^{99m}Tc-MDP after 4 h. ($n=3$)

Post-injection (IV administration) scans of ^{99m}Tc-MDP-SLNs in rats showed that, the emulsion moved via the blood circulation and deposited the highest in the following organs; kidneys (3.87%ID/g), bone (2.66%ID/g), small intestines (0.59%ID/g) and stomach (0.55%ID/g). The least amount of deposition was in the heart (0.18%ID/g) and liver (0.14%ID/g). The biodistribution and clearance profile of ^{99m}Tc-MDP was similar to that displayed by the SLN formulation (Figure 3). Similarly a high deposition of the ^{99m}Tc-MDP compound was observed in the kidneys (3.07%ID/g) and bone (1.95%ID/g). The following organs reported the least amounts of deposition; liver (0.05%ID/g), muscle (0.05%ID/g), heart (0.10%ID/g), spleen (0.12%ID/g), lungs (0.17%ID/g) and stomach (0.17%ID/g). These compounds localized in the bone due to the fact that ^{99m}Tc-MDP is a bone seeking agent and will advertently accumulate in bone and soft tissue. Thereafter they are excreted via the kidneys and bladder. Intravenously administered ^{99m}Tc-MDP is expected to rapidly clear from the blood and accumulate in bone (Geskovski *et al.,* 2013). The remaining ^{99m}Tc-MDP is excreted via the kidney in urine (Geskovski *et al.,* 2013).

High absorption of the SLNs was reported in the kidneys, bone and GI tract followed by the spleen. Although high absorption was observed in the kidneys and bone, trace amounts in the stomach, spleen, small and large intestines prove that sufficient amounts of ^{99m}Tc-MDP was encapsulated. Rapid excretion was observed via the bladder, although ^{99m}Tc-MDP clearance was faster. It was expected and hypothesised that the application of SLN would reduce accumulation of the encapsulated ^{99m}Tc-MDP in organs and bone. However, the SLN delivery system similarly showed rapid excretion of the encapsulated ^{99m}Tc-MDP (SLN) as ^{99m}Tc-MDP. There was however, no great difference in biodistribution between the ^{99m}Tc-MDP and ^{99m}Tc-MDP-SLNs post intravenous administration. Therefore, it's unclear whether what was observed was the SLNs or ^{99m}Tc-MDP and ^{99m}Tc-MDP probably influences the distribution of SLNs and possibly influences its own release rate. It is not clear whether SLNs (IV) distributed to organs or whether it released the ^{99m}Tc-MDP.

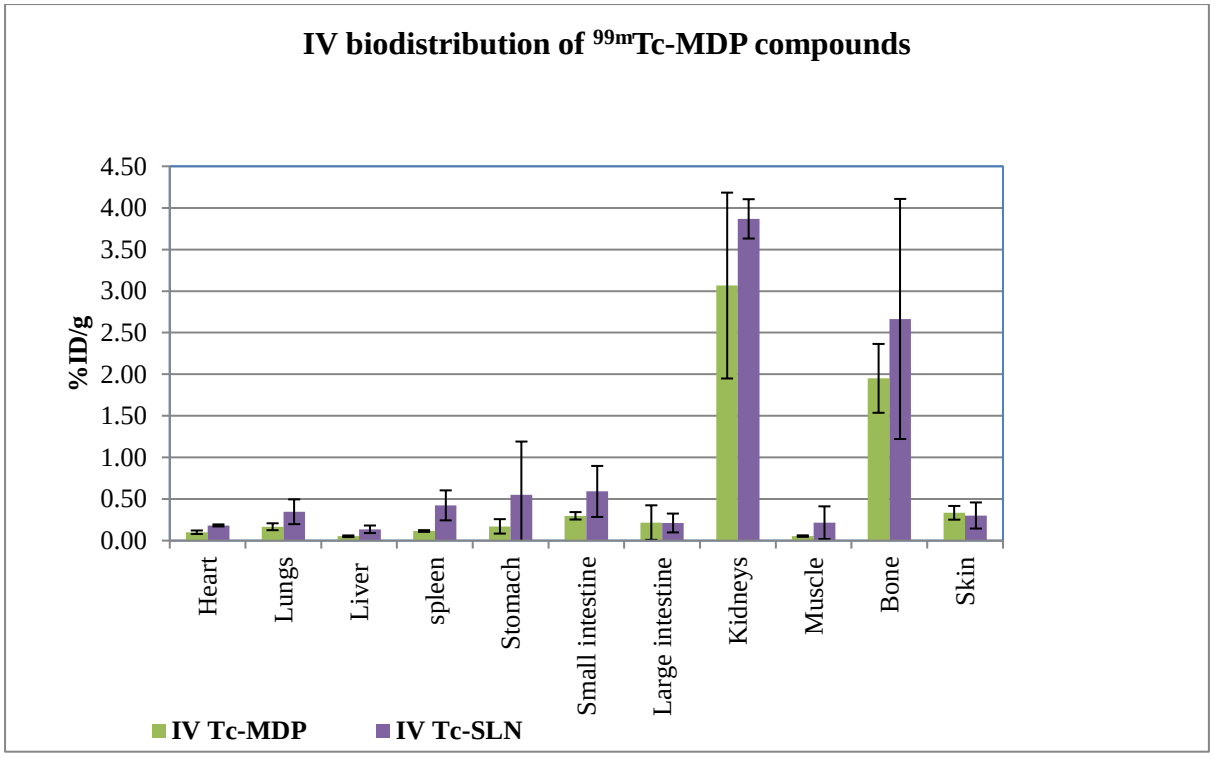

Fig. 3. The *in vivo* biodistribution of intravenously injected ^{99m}Tc-MDP solid lipid nanoparticles and ^{99m}Tc-MDP after 4 h. (*n=3*)

A comparative illustration of the organs which had the highest and lowest deposition of ^{99m}Tc-MDP-SLNs and ^{99m}Tc-MDP is shown in Figure 4. The orally ingested ^{99m}Tc-MDP-SLNs reported the highest localisation of nanoparticles in the kidneys (8.50%ID/g) and stomach (8.04%ID/g). The same ingested SLNs incurred the least amount of deposition in the heart (0.12%ID/g), spleen (0.13%ID/g) and muscle (0.18%ID/g). Similarly, ingested ^{99m}Tc-MDP had great localisation in the large intestines (7.08%ID/g), kidneys (1.71%ID/g), small intestines (1.46%ID/g) and stomach (1.10%ID/g). The liver (0.24%ID/g) and spleen (0.42%ID/g) had the least amount of ^{99m}Tc-MDP deposition.

The injected ^{99m}Tc-MDP-SLNs also showed a high localisation of particles in the kidneys (3.87%ID/g) followed by bone (2.66%ID/g) accumulation. The intravenous control group ^{99m}Tc-MDP also exhibited the highest deposition in the kidneys (3.07%ID/g) and bone (1.95%ID/g). Both these compounds reported significantly low deposition values in the heart, liver and spleen.

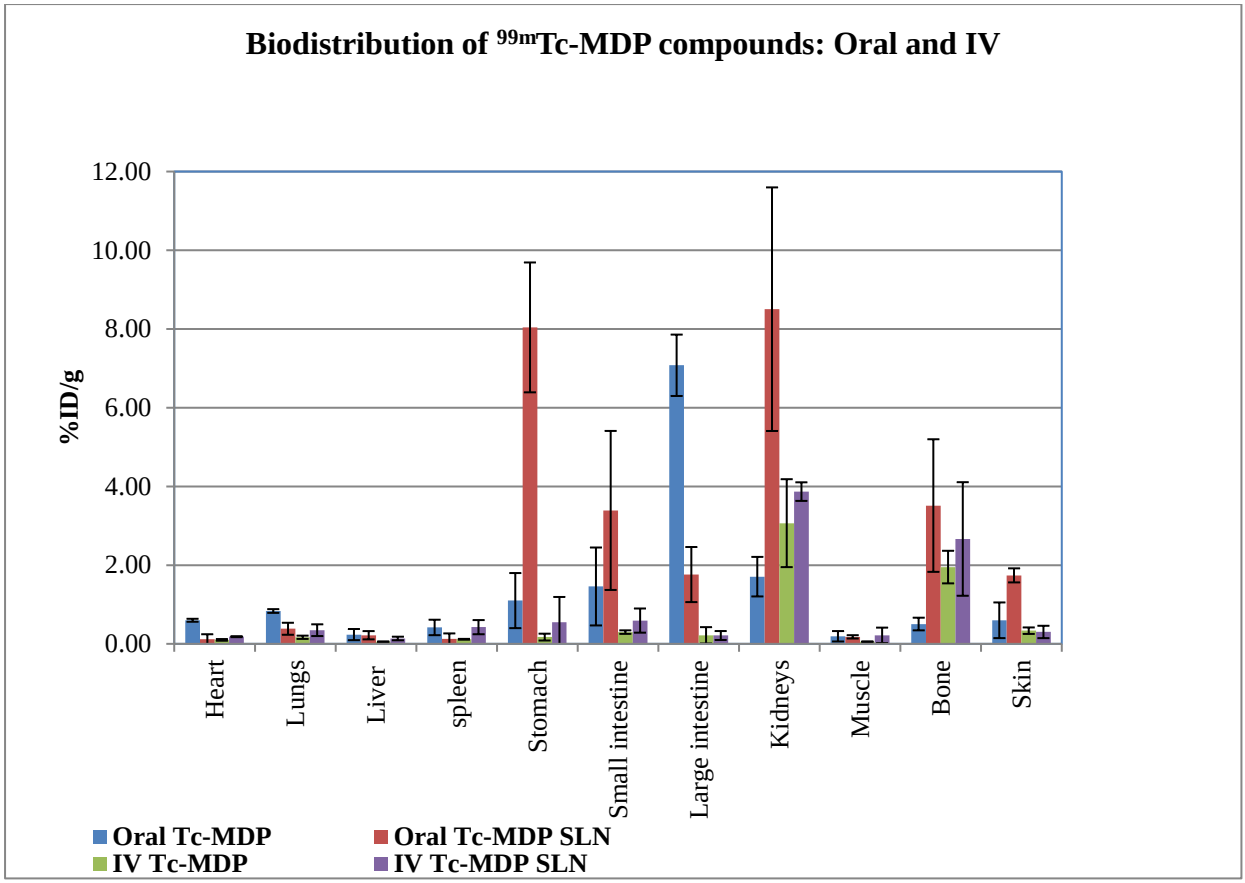

Fig. 4. A comparative biodistribution of orally ingested and injected ^{99m}Tc-MDP-SLNs and ^{99m}Tc-MDP after 4 h. (*n=3*)

4. Conclusion

The distribution determination of the encapsulated ^{99m}Tc-MDP in SLNs was successful, however not as was hypothesized. The *in vivo* biodistribution of radiolabelled ^{99m}Tc-MDP-SLNs in tissue at a 4 h time point after intravenous and oral administration was confirmed by observation of the radiolabelled nanoparticle compounds under a single photon emission tomography/computed tomography (SPECT/CT) gamma camera.

Orally administered SLN delivery systems changed the biodistribution of encapsulated ^{99m}Tc-MDP enabling the transport of ^{99m}Tc-MDP over the gut membrane and subsequent delivery to other organs such as bone. There was however, no significant difference in biodistribution between intravenously injected ^{99m}Tc-MDP and ^{99m}Tc-MDP-SLNs. Based on these studies the use of SLNs, if optimised to avoid non-target uptake, can be further investigated for its potential

to enable the oral administration of ^{99m}Tc based radiopharmaceuticals as compared to its conventional intravenous form of administration.
Some evidence was also found that for intravenously administrated ^{99m}Tc-MDP-SLNs, the apparent clearance of the radiopharmaceutical from the body was reduced or delayed.

Conflict of interest

Conflict of interest: none.

Acknowledgements

The authors would like to thank the Nuclear Technologies in Medicine and the Biosciences Initiative (NTeMBI), for their funding. It's a national technology platform developed and managed by the South African Nuclear Energy Corporation (Necsa) and funded by the Department of Science and Technology. A special thanks to Kobus Venter (Medical Research Council) for assisting with the animal handling and management and Cindy Els and Delene van Wyk at the Steve Biko Academic Hospital for assisting with the scintigraphic imaging. The authors would also like to acknowledge the entire NTeMBI consortium composed of and including the Council for Scientific and Industrial Research (CSIR), Necsa, DST/NWU Preclinical Drug Development Platform at the North West University (NWU) and Medical Research Council (MRC).

Funding

This work was supported by the Nuclear Technologies in Medicine and the Biosciences Initiative (NTeMBI). It's a national technology platform developed and managed by the South African Nuclear Energy Corporation (Necsa) and funded by the Department of Science and Technology. NTeMBI had no direct involvement in conducting the research or in the writing of this article.

References

Almeida, A.J. and Souto, E., 2007. Solid lipid nanoparticles as a drug delivery system for peptides and proteins. Advanced Drug Delivery Reviews 59, 478–490.

Bhatnagar, A., Hustinx, R. and Alavi, A., 2000. Nuclear imaging methods for non-invasive drug monitoring. Advanced drug delivery reviews 41, 41–54.

Chopra, D., 2011. Radiolabelled Nanoparticles for Diagnosis and Treatment of Cancer, Radioisotopes- Applications in Bio-Medical Science, Prof. Nirmal Singh (Ed.), ISBN: 978-953-307-748-2, inTech, Available from: http://www.intechopen.com/books/radioisotopes-applications-in-bio-medical-science/radiolabelled-nanoparticles-for-diagnosis-and-treatment-of-cancer.

Ekambaram, P., Abdul Hasan Sathali, A. and Priyanka K., 2012. Solid lipid nanoparticles: A review. Scientific Reviews and Chemical Communications 2(1), 80-102.

Geskovski, N., Kuzmanovska, S., Crcarevska, M.S., *et al*., 2013. Comparative biodistribution studies of technetium-99m radiolabeled amphiphilic nanoparticles using three different reducing agents during the labelling procedure. Journal of Labelled Compounds and Radiopharmaceuticals 56, 689-695.

Lasoń, E., Ogonowski, J. and Chemistry, O., 2011. Solid Lipid Nanoparticles- characteristics, application and obtaining 45 years of FCE & T of Cracow University of Technology. Chemik 65(10), 960-967.

Mandiwana, V., Kalombo, L., Venter, K. *et al.*, 2015. Samarium oxide as a radiotracer to evaluate the *in vivo* biodistribution of PLGA nanoparticles. Journal. Nanoparticle .Research 17, 1-11 http://dx.doi.org/10.1007/s11051-015-3182-3

Mehnert, W. and Mäder, K., 2001. Solid lipid nanoparticles production, characterisation and applications. Advanced Drug Delivery Reviews 47, 165-197.

Mitterhauser, M., Wadsak, W., Eidherr, H. *et al*., 2004. Labelling of EDTMP (Multibone) with [^{111}In], [^{99m}Tc] and [^{188}Re] using different carriers for "cross complexation." Applied Radiation and Isotopes 60, 653-658.

Munireddy, M., Thakur, R.S., Patel, R. and Mamatha M.C., 2012. Solid Lipid Nanoparticles : An Effective Drug Delivery System- A Review 2(3), 9-27.

Parhi, R. and Suresh, P., 2012. Preparation and characterisation of solid lipid nanoparticles- A review. Current Drug Discovery Technologies 9, 2-16.

Parveen, S., Misra, R. and Sahoo, S.K., 2012. Nanoparticles: a boon to drug delivery, therapeutics, diagnostics and imaging. Nanomedicine: Nanotechnology, Biology and Medicine 8, 147-166.

Perkins, A.C. and Frier, M., 2004. Radionuclide imaging in drug development. Bentham Science Publishers Ltd, Current Pharmaceutical Design 10, 2907-2921.

Ramteke, K.H., Joshi, S.A. and Dhole, S.N., 2012. Solid Lipid Nanoparticle : A Review. Journal of Pharmacy 2(6), 34-44.

Sheets, N.C. and Wang, A.Z., 2011. Radioisotopes and Nanomedicine. Radioisotopes-Applications in Bio-Medical Science, (Bangham 1993), 47-66. Available at: http://www.intechopen.com/books/radioisotopes-applications-in-bio-medical-science/radioisotopes-and-nanomedicine.

Truluck, C.A., 2007. Nuclear medicine technology: Inflammation and infection imaging. Journal of Radiological Nursing 26, 77-85.

Wissing, S. A., Kayser, O. and Müller, R.H., 2004. Solid lipid nanoparticles for parenteral drug delivery. Advanced Drug Delivery Reviews 56, 1257-1272.

Yeong, C.H., Blackshaw, P.E., Ng, K.H., *et al*., 2011. Reproductivity of neutron activated Sm-153 oral dose formulations intended for human administration. Applied Radiation and Isotopes 69(9), 1181-1184.